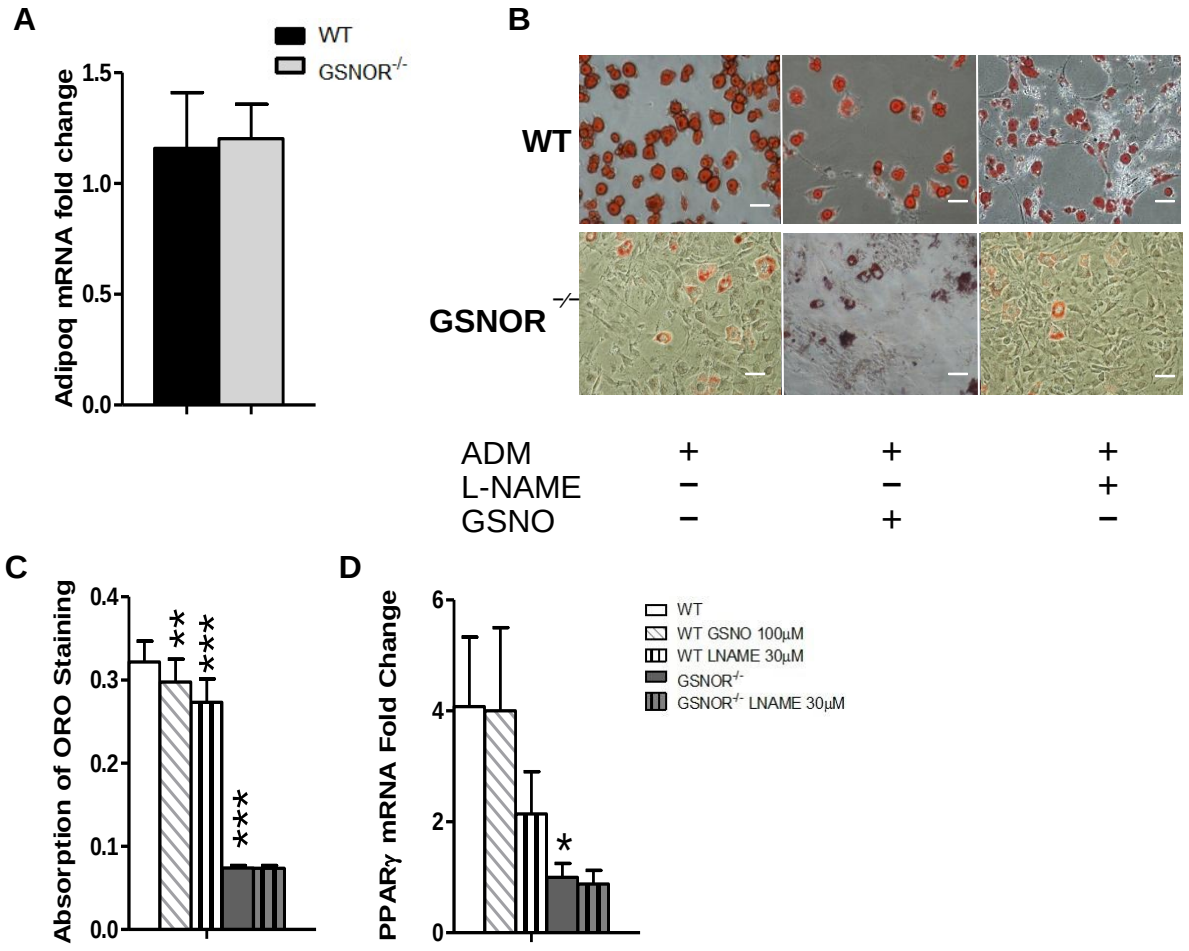

Figure S1. (A) Expression of *Adiponectin (Adipoq)* in WT and GSNOR$^{-/-}$ BMMSCs cultured with adipogenic medium. n=3. **(B)** Oil Red O staining of WT BMMSCs grown in adipogenic medium and treated with NO donor GSNO (100μM), or pan-NOS inhibitor L-NAME (30μM) for 2 weeks and GSNOR$^{-/-}$ BMMSCs treated with L-NAME. Scale Bar: 100μm. **(C)** Oil Red O staining was quantified and normalized to baseline staining. **(D)** Expression of *PPARγ* after drug treatment. n=3 per group (A-C). * P<0.05, ** P<0.01, *** P<0.001 compared to WT, analyzed by two way ANOVA, Bonferroni's multiple comparison test. Statistical significance between two groups was determined by student's t-test (2-tailed) and presented as mean ± SEM.

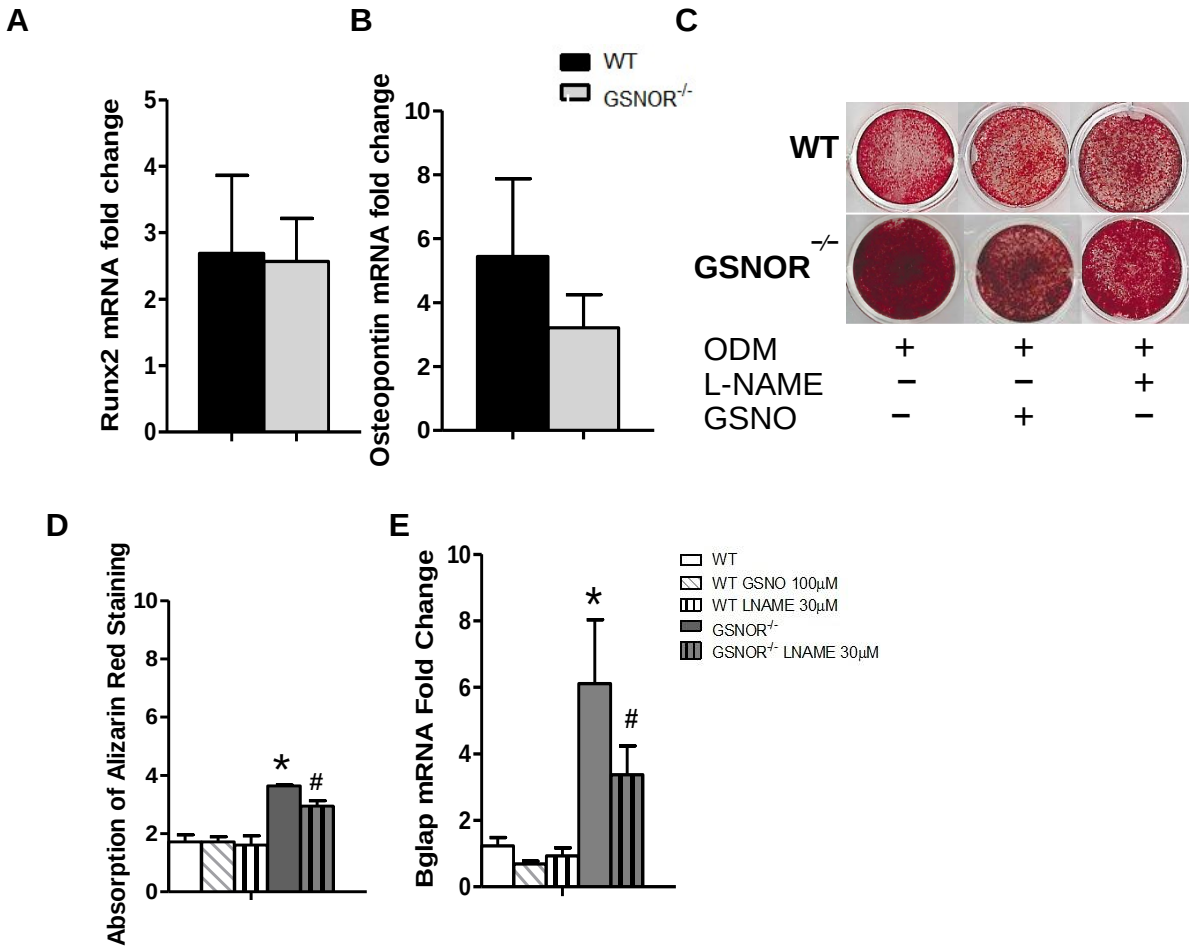

Figure S2. (A,B) Expression of *Runx2* **(A)** and *Spp1* (*Osteopontin*) **(B)** in WT and GSNOR$^{-/-}$ BMMSCs cultured with osteogenic medium. n=3. **(C,D)** WT BMMSCs were grown in osteogenic medium and treated with NO donor GSNO (100μM), or pan-NOS inhibitor L-NAME (30μM) for 2 weeks. GSNOR$^{-/-}$ BMMSCs were treated with L-NAME. Alizarin Red-S staining was performed **(C)** and quantified **(D)**. **(E)** Cells were treated similarly in C and D and expression of *Bglap* assessed by quantitative real-time RT-PCR analysis. n=3 per group (D,E). * P<0.05 compared to WT, # P<0.05 compared to GSNOR$^{-/-}$, analyzed by two way ANOVA, Bonferroni's multiple comparison test. Statistical significance between two groups was determined by student's t-test (2-tailed) and presented as mean ± SEM.

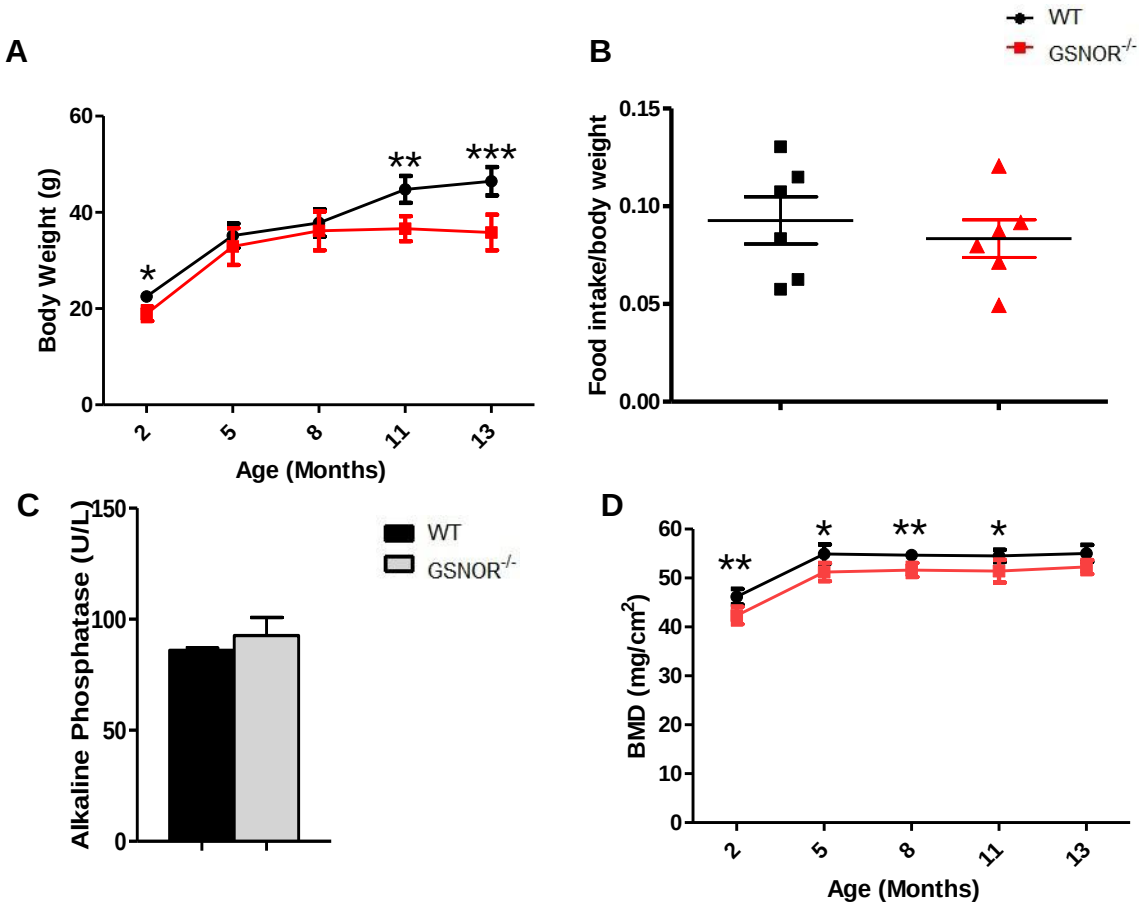

Fig S3. (A) Body weight of WT and GSNOR$^{-/-}$ mice over a course of 13 months. n=6 (WT) and n=4 (GSNOR$^{-/-}$). **(B)** Food intake of WT and GSNOR$^{-/-}$ mice measured in metabolic cage. n=6. **(C)** Serum levels of alkaline phosphatase were not altered in GSNOR$^{-/-}$ mice. n=3. **(D)** Bone mineral density of WT and GSNOR$^{-/-}$ mice over a course of 13 months. n=6 (WT) and n=4 (GSNOR$^{-/-}$). * P<0.05, ** P<0.01, *** P<0.001 compared to WT at corresponding age, analyzed by two way ANOVA, Bonferroni's multiple comparison test. Statistical significance between two groups was determined by student's t-test (2-tailed) and presented as mean ± SEM.

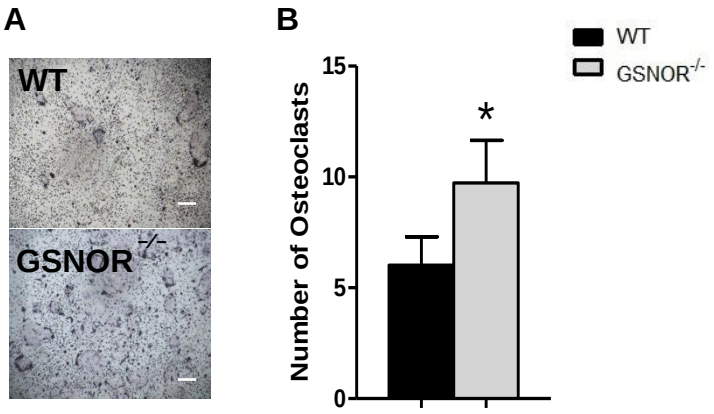

Fig S4. GSNOR$^{-/-}$ BMMNCs have enhanced osteoclast differentiation *in vitro*. **(A)** TRAP staining of WT and GSNOR$^{-/-}$ cells. Scale Bar: 100µm. **(B)** The number of TRAP-positive osteoclasts was quantitated. n=3, * P<0.05 compared to WT. Statistical significance was determined by unpaired student's t-test (2-tailed) and presented as mean ± SEM.

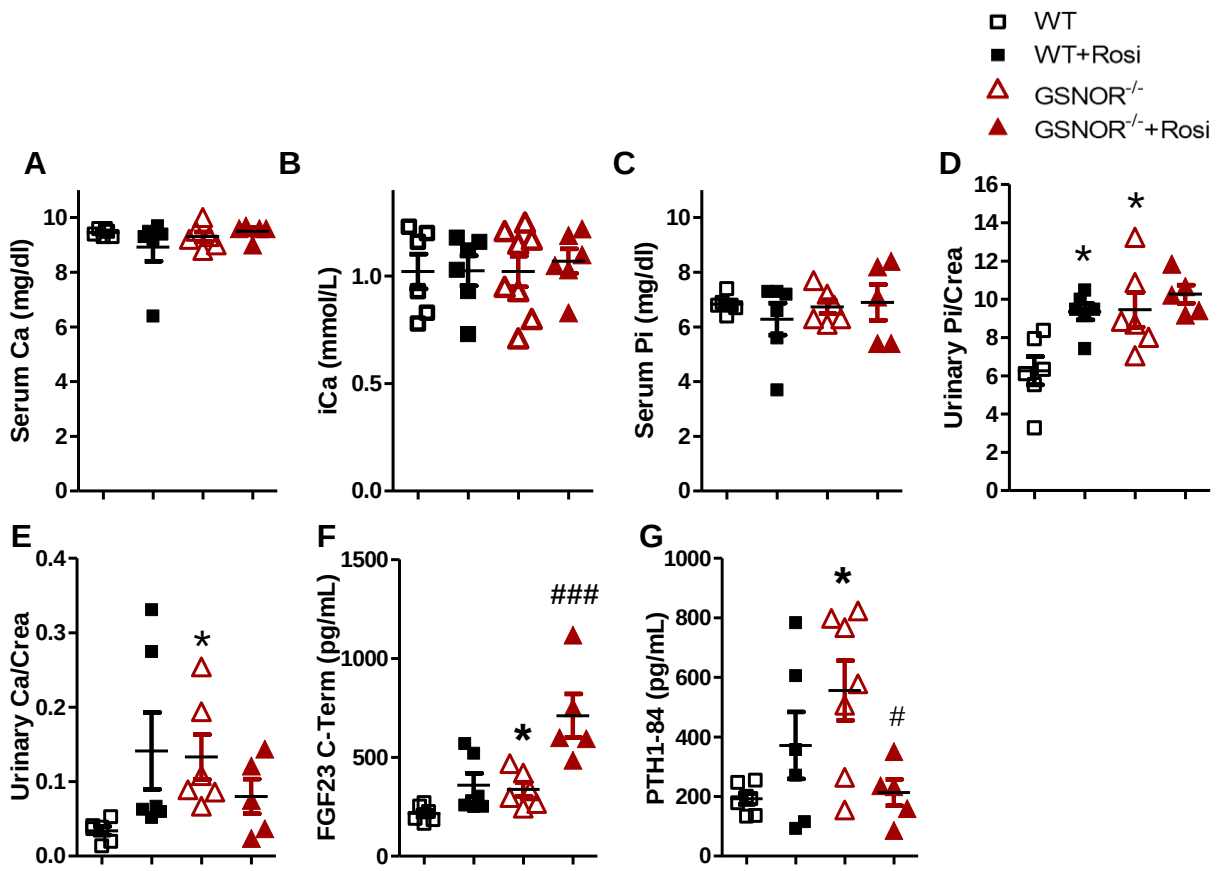

Fig S5. GSNOR$^{-/-}$ mice have altered calcium and phosphate hormonal regulation. **(A, B)** Serum calcium level **(A)** and ionized calcium (iCa) level **(B)** in 2-month-old male WT and GSNOR$^{-/-}$ mice. **(C)** Serum phosphate level in 2-month-old male WT and GSNOR$^{-/-}$ mice. **(D)** Urine phosphate/ urine creatinine ratio. n=5-6. **(E)** Urine calcium/ urine creatinine ratio. **(F)** Serum FGF23 level. **(G)** Serum PTH level. Statistical significance was determined by two-way ANOVA and presented as mean ± SEM. n=5-7. * P<0.05 compared to WT, # P<0.05 compared to GSNOR$^{-/-}$, ### P<0.001 compared to GSNOR$^{-/-}$ analyzed by Bonferroni's multiple comparison test.

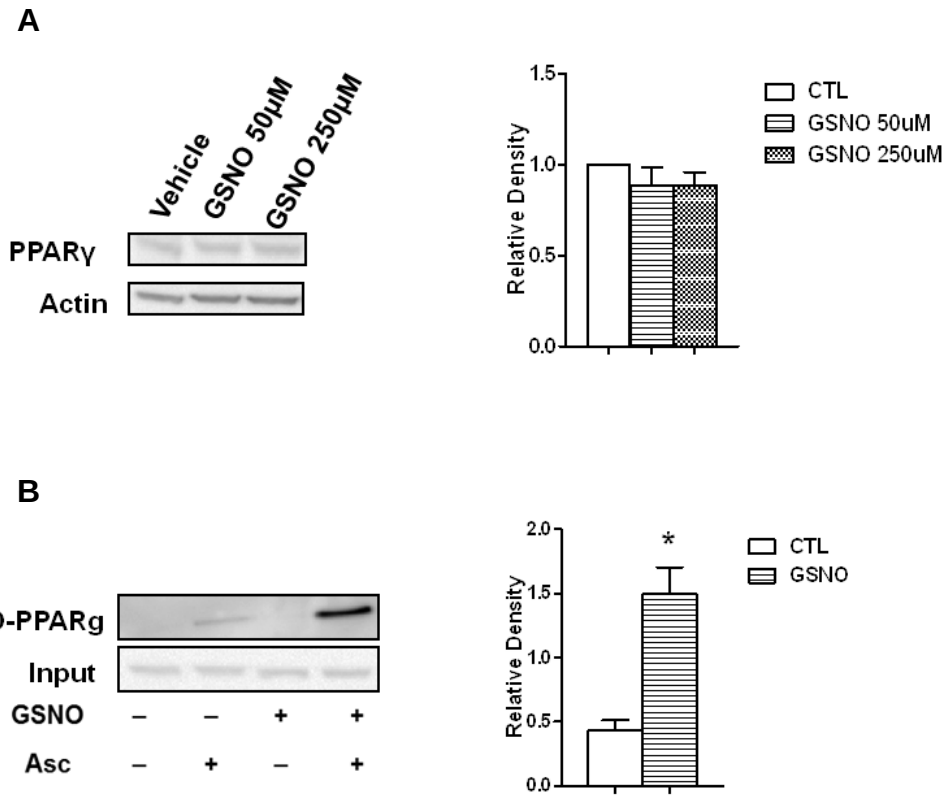

Fig S6. PPARγ expression and S-nitrosylation after GSNO treatment in HEK-293T cells. **(A)** PPARγ protein expression in HEK-293T cells after GSNO treatment. **(B)** PPARγ protein S-nitrosylation in HEK-293T cells measured by SNO-RAC after GSNO treatment. Asc: Ascorbic Acid. n=3, *P<0.05 compared to no GSNO treatment control. Statistical significance between two groups was determined by unpaired student's t-test (2-tailed) and presented as mean ± SEM.

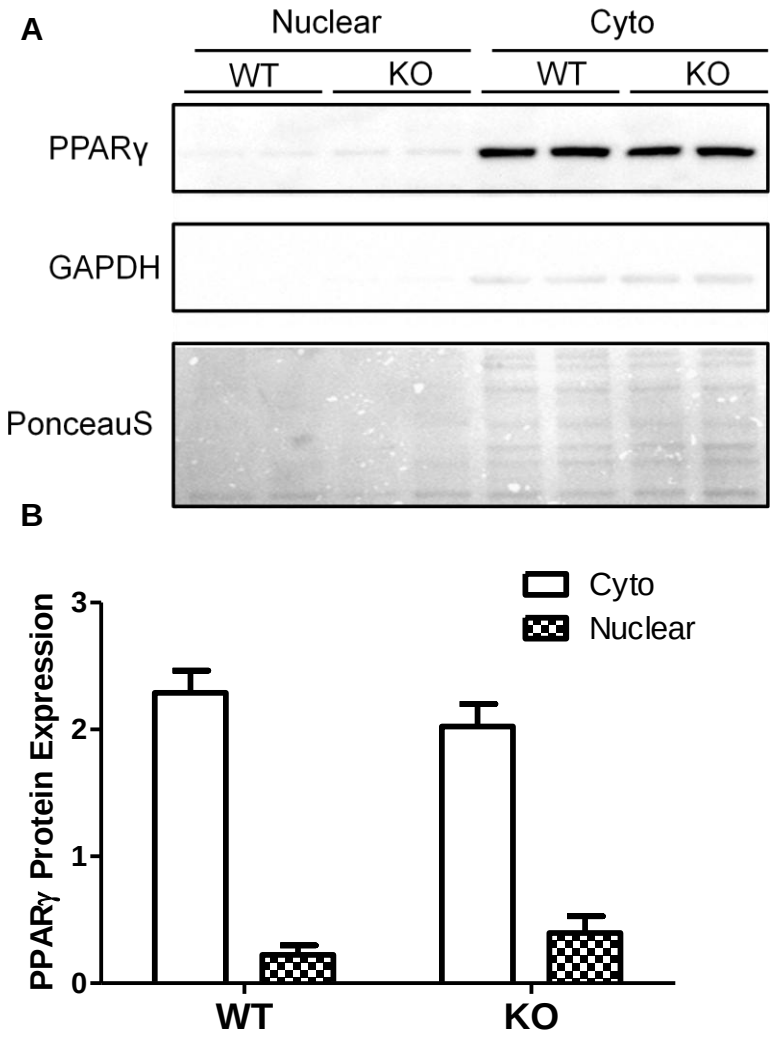

Figure S7. Cytoplasmic and nuclear expression of PPARγ. (A) Cytoplasmic and Nuclear localization of PPARγ in WT and GSNOR$^{-/-}$ MSCs. **(B)** Quantification of PPARγ localization. n=4. (Nuclear protein loading:6.5µg, Cytoplasm protein loading: 12.5µg)

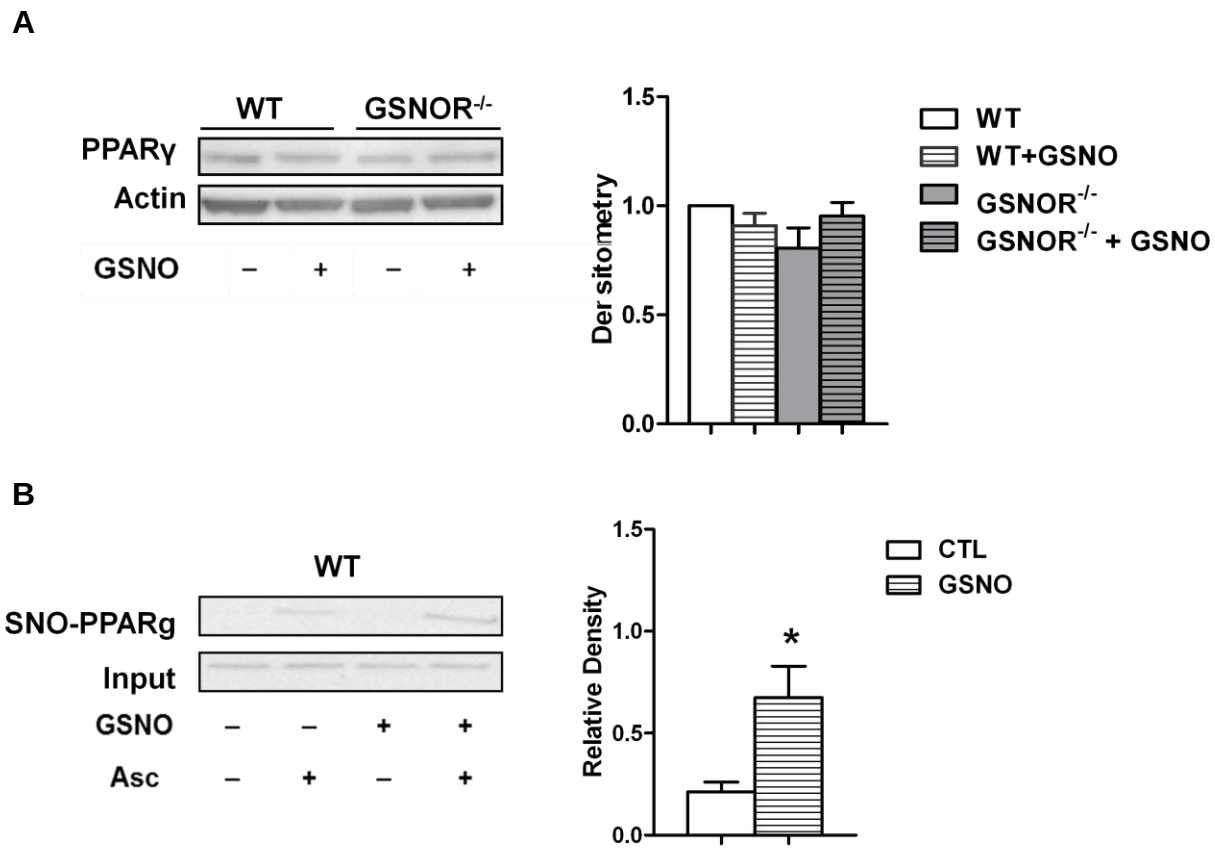

Fig S8. PPARγ expression and S-nitrosylation after GSNO treatment in WT MSCs. **(A)** PPARγ protein expression in WT and GSNOR$^{-/-}$ MSCs after GSNO treatment. **(B)** PPARγ protein S-nitrosylation in WT MSCs measured by SNO-RAC after GSNO treatment. Asc: Ascorbic Acid. n=3, *P<0.05 compared to no GSNO treatment control. Statistical significance between two groups was determined by unpaired student's t-test (2-tailed) and presented as mean ± SEM.

A

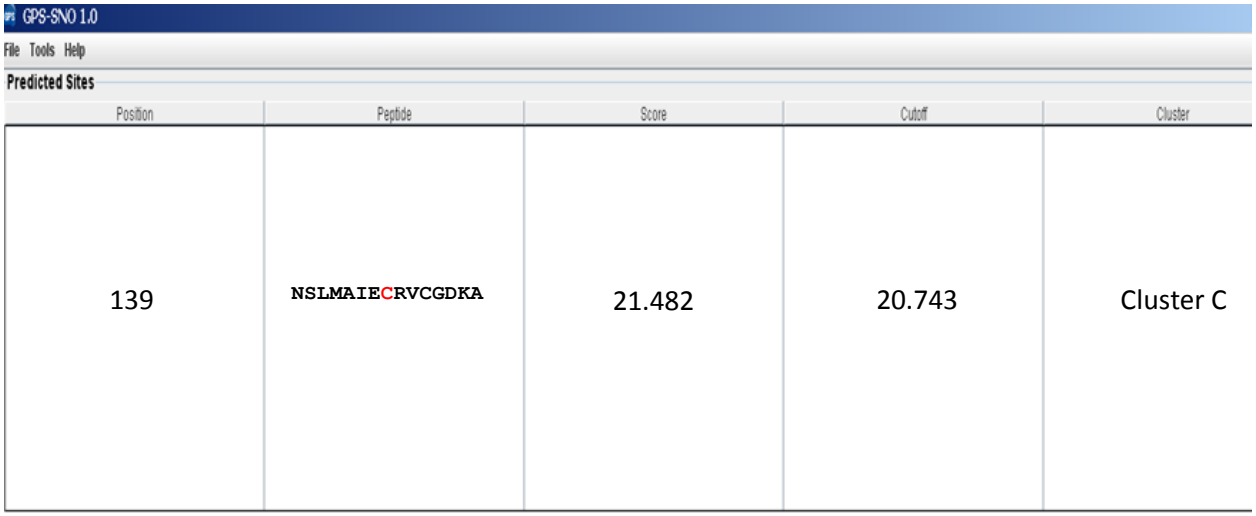

B

SNSLMAIECRVCGDKASGFHYGVHACEGCKGF

Fig S9. Sequence of S-nitrosylation site of PPARγ was analyzed. There are ten potential cysteine residues (Cys) in PPARγ sequence. A software, GPS-SNO 1.0, was used to predict the S-nitrosylation site (1). No cysteine was identified using high threshold and Cys139 was identified under medium threshold. **(A)** Identification of Cys 139 with GPS-SNO 1.0. **(B)** Illustration of three cysteine targets: Cys 139, Cys 156 and Cys 159 labeled in red.

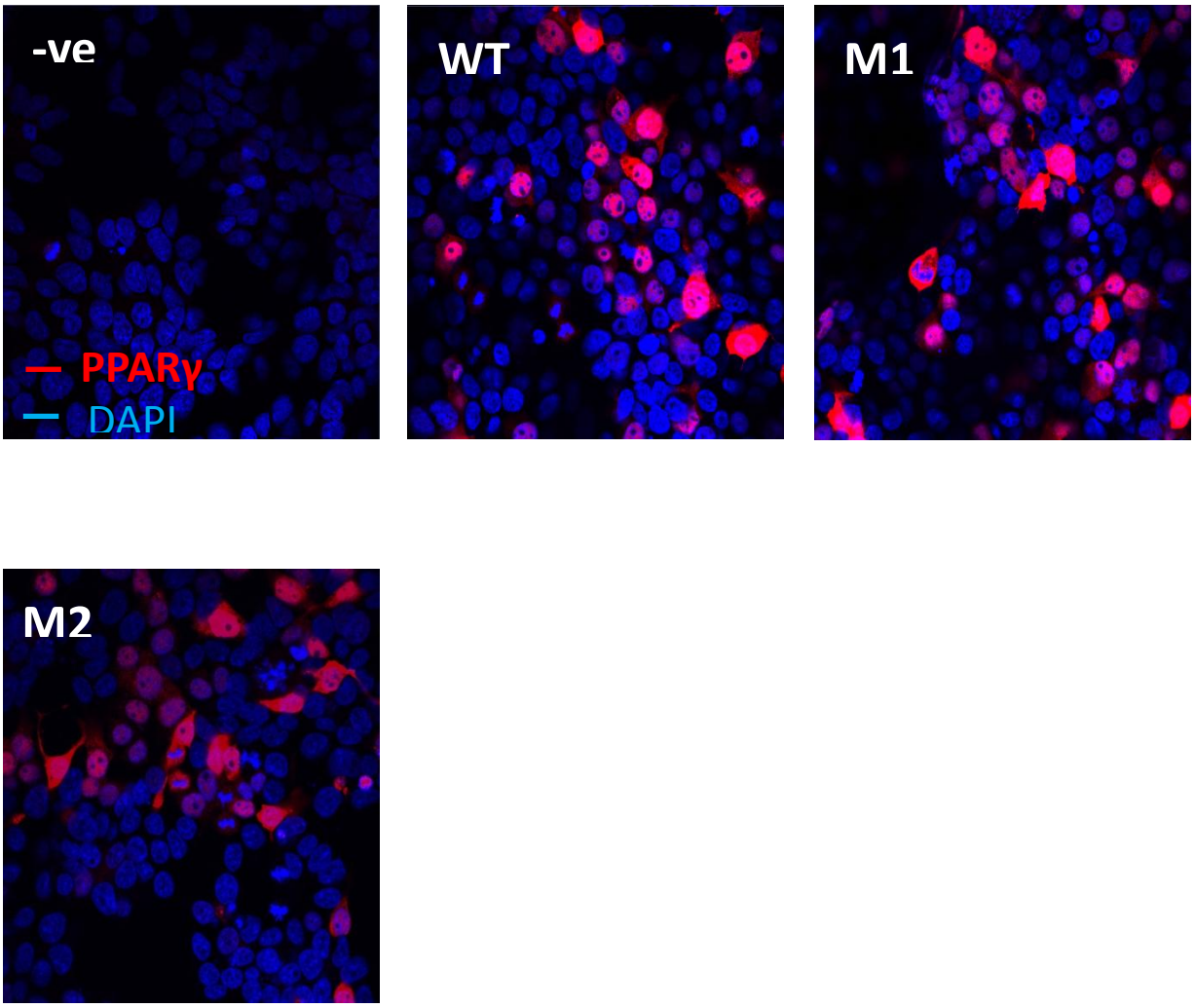

Fig S10. Sub-cellular localization of wild type and two PPARγ mutants (M1, M2) in HEK-293T cells.

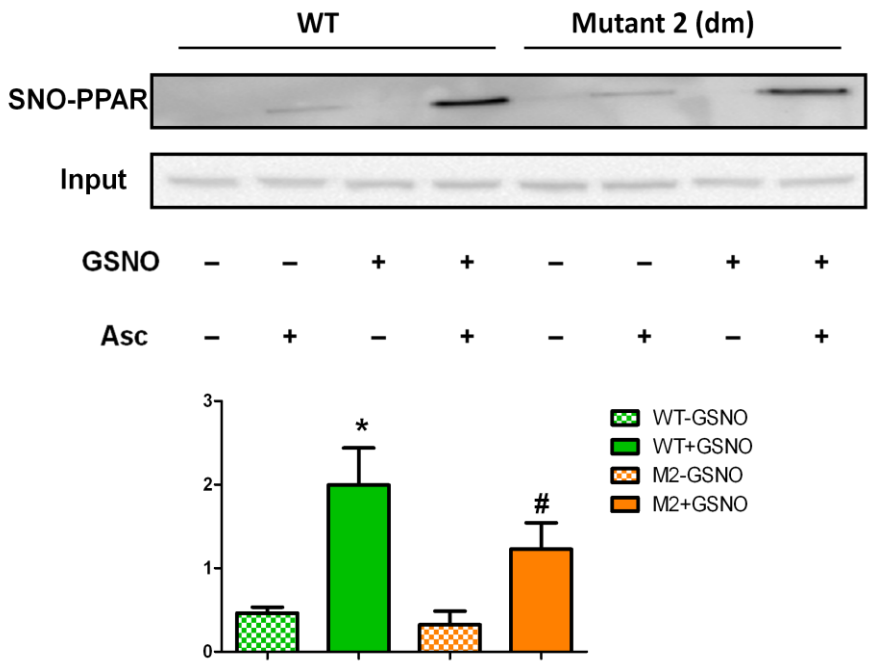

Figure S11. SNO-PPARγ in HEK-293T cells overexpressed with WT and mutant 2 (double mutant: Cys 156/159), measured by SNO-RAC. Asc: Ascorbic Acid. Omission of ascorbic acid were used to as negative controls.* P<0.05 compared to overexpression of WT PPARγ and without GSNO treatment, # P<0.05 compared to overexpression of M2 PPARγ and without GSNO treatment, analyzed by Bonferroni's multiple comparison test (2-way ANOVA, for GSNO treatment P=0.0024), n=5. Data was presented as mean ± SEM.

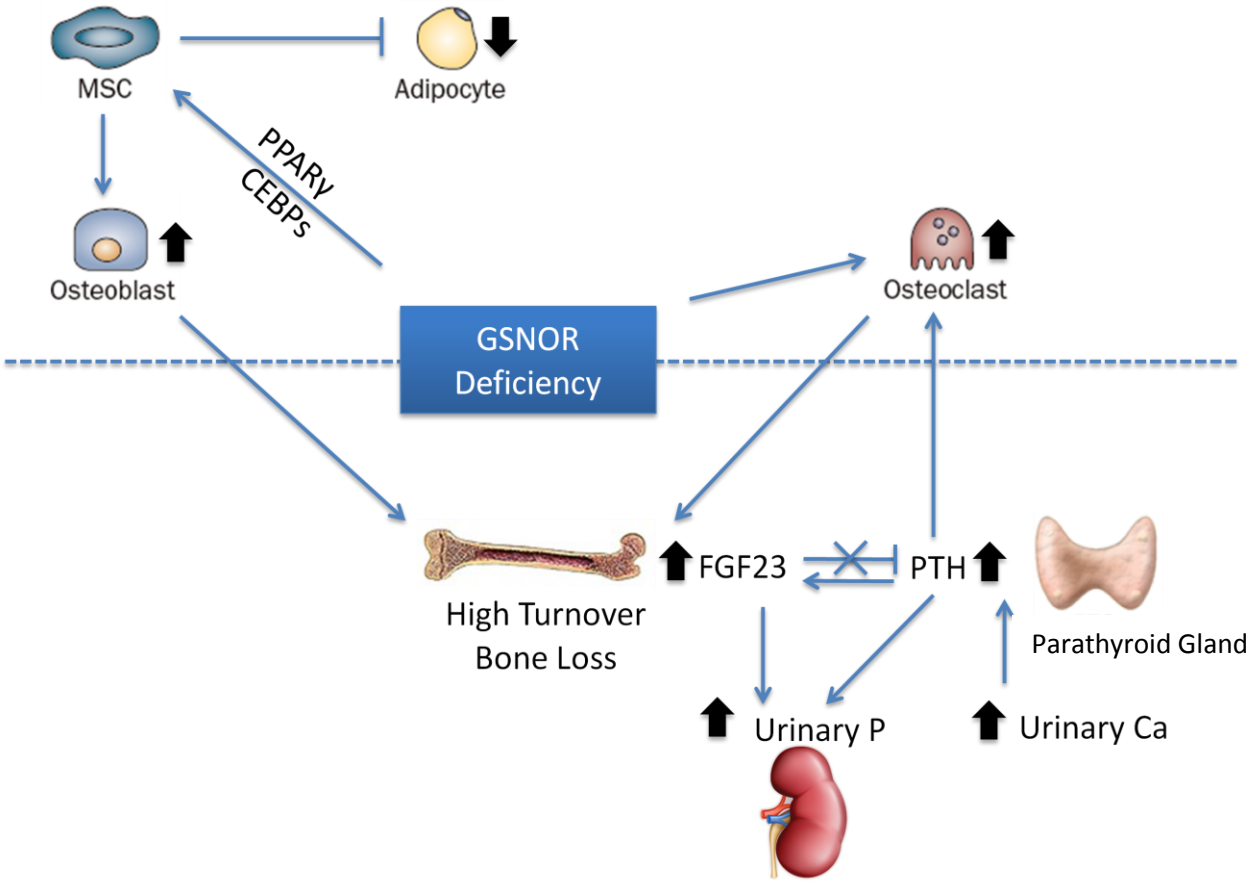

Figure S12. The adipose-skeletal phenotypes of mice with GSNOR deficiency. GSNOR$^{-/-}$ MSCs have decreased adipogenesis and increased osteoblast differentiation due, at least in part, to increased S-nitrosylation of PPARγ. Despite increased osteoblast formation from MSCs, GSNOR$^{-/-}$ mice have diminished bone density. This phenotype is associated with increased osteoclast differentiation, and elevated urinary excretion of both phosphate and calcium. In addition, there is elevated FGF23 and PTH in the animal. This phenotype suggests that other endocrine or renal mechanisms may participate in the bone loss of the GSNOR$^{-/-}$ mice. Parts of the artwork were derived from references (2;3).

Variable	WT	GSNOR$^{-/-}$	P value
Structure			
BV/TV (%)	14.37±1.35	9.951±0.84	0.025
Tb. N	3.82±0.16	2.81±0.27	0.0054
Tb. Th (µm)	37.36±2.67	35.76±0.92	NS
Tb. Sp (µm)	227.90±12.39	341.90±43.66	0.014
Formation			
Ob.S/BS (%)	0.997±0.21	4.82±0.94	0.0007
N.Ob/B.Pm	0.73±0.15	3.35±0.67	0.0009
MS/BS (%)	5.93±0.92	10.49±1.66	0.0246
MAR (µm/d)	0.91±0.09	1.27±0.09	0.026
BFR/BS ($\mu m^3 \mu m^2$/d)	19.18±3.41	50.22±10.76	0.0092
OV/BV (%)	0.31±0.16	3.25±0.36	<0.0001
OS/BS (%)	3.89±1.23	21.61±2.10	<0.0001
Resorption			
ES/BS (%)	2.25±0.51	5.53±1.03	0.0091
Oc.S/BS (%)	0.87±0.21	2.22±0.38	0.0057
N.Oc/B.Pm	0.32±0.07	0.88±0.16	0.004

Table S1. Histomorphometric analysis of femur from WT and GSNOR$^{-/-}$ mice. n=8 (WT) and n=6 (GSNOR$^{-/-}$).

Variable	WT	GSNOR$^{-/-}$	P value
Trabecular parameters			
BV/TV (%)	13.00±0.64	5.748±0.93	0.0003
BMD	0.47±0.062	0.57±0.24	NS
Tb. N	0.0023±8.029x10^{-5}	0.0012±0.00016	0.0003
Tb. Th (µm)	56.30±1.267	48.32±1.299	0.0034
Tb. Sp (µm)	224.1±4.870	289.3±15.80	0.0033
Cortical parameters			
BMD	1.667±0.020	1.593±0.004	0.0148

Table S2. µCT analysis of femur from WT and GSNOR$^{-/-}$ mice. n=5 (WT) and n=4 (GSNOR$^{-/-}$).

Supplemental Experimental Procedures

Osteoclast differentiation. Bone marrow mononuclear cells (BMMNCs) were generated by culturing bone marrow cells with mouse colony stimulating factor (25ng/ml M-CSF, Sigma). BMMNCs were cultured in osteoclastogenic differentiation medium (containing 25ng/ml M-CSF and 100ng/ml RANKL, Millipore) for 6 days and TRAP staining was conducted using the TRAP kit (Sigma) according to the manufacturer's instructions. The number of TRAP positive osteoclasts was counted using Image J software (National Institutes of Health).

Immunofluorescence. Cells were fixed in 4% paraformaldehyde, permeabilized, and blocked with 0.3%TritonX-100, 1%BSA, and10%normal donkey serum in PBS at room temperature for 45min. Cells were then incubated with primary antibodies: rabbit PPARγ mAb (Cell Signaling) overnight at 4°C and then with anti-rabbit 568-conjugated secondary antibodies (Invitrogen) for 1 h in the dark at room temperature. Nuclear labeling was obtained with DAPI. The slides were mounted in Prolong Gold anti-fade reagent (Invitrogen). Images were obtained using a Zeiss LSM-710 confocal microscope (Analytical Imaging Core Facility, University of Miami). A negative control (PBS containing 1% BSA and 10% donkey serum with no primary antibody) was included in every experiment.

Nuclear and cytoplamic protein extraction. Extraction was performed according to the protocol of NE-PER Nuclear Protein Extraction Kit (Pierce).

Reference List

1. Xue,Y., Liu,Z., Gao,X., Jin,C., Wen,L., Yao,X., and Ren,J. 2010. GPS-SNO: computational prediction of protein S-nitrosylation sites with a modified GPS algorithm. *PLoS. One.* **5**:e11290.
2. Takada,I., Kouzmenko,A.P., and Kato,S. 2009. Wnt and PPARgamma signaling in osteoblastogenesis and adipogenesis. *Nat. Rev. Rheumatol.* **5**:442-447.
3. Quarles,L.D. 2008. Endocrine functions of bone in mineral metabolism regulation. *J. Clin. Invest* **118**:3820-3828.

Figure 5A uncut gel

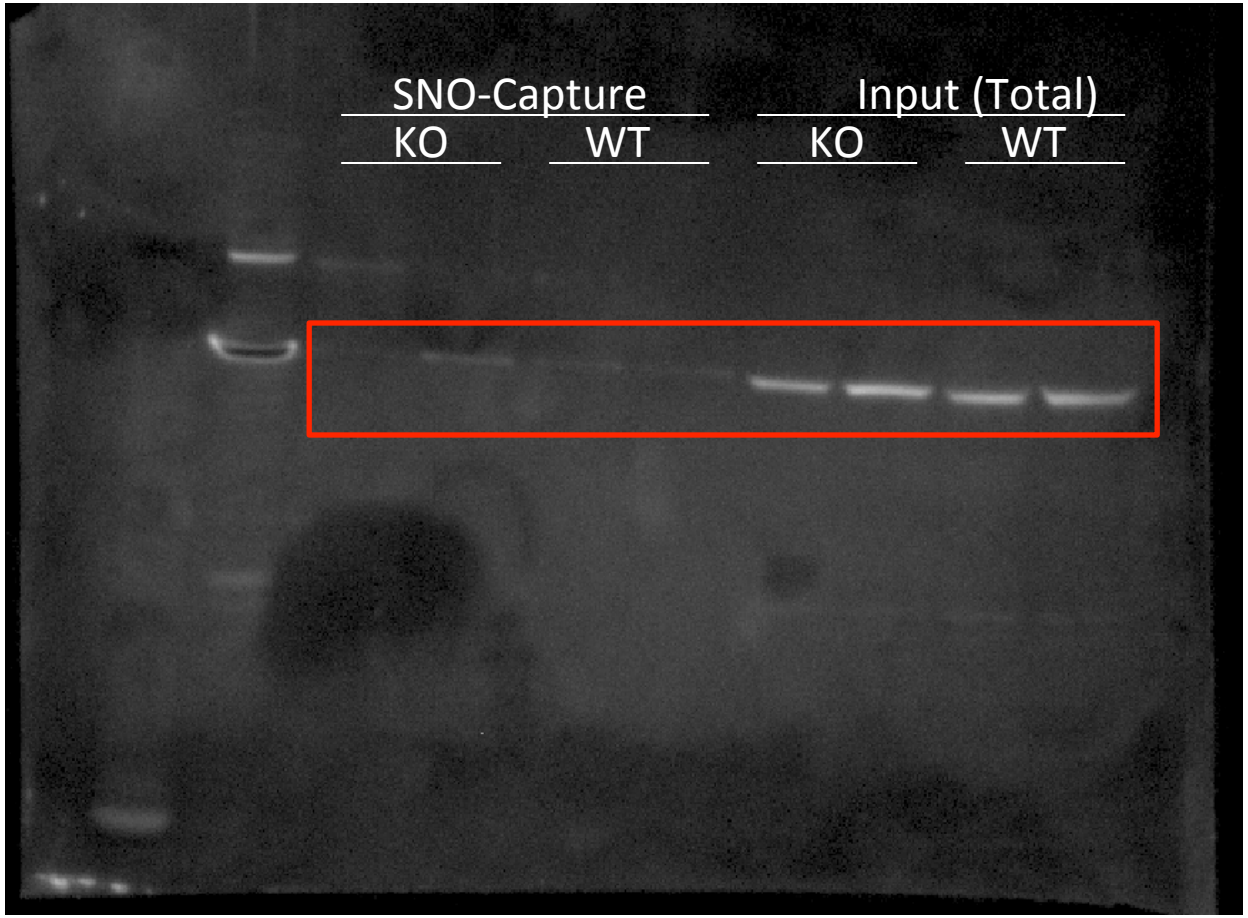

Figure 5C uncut gel

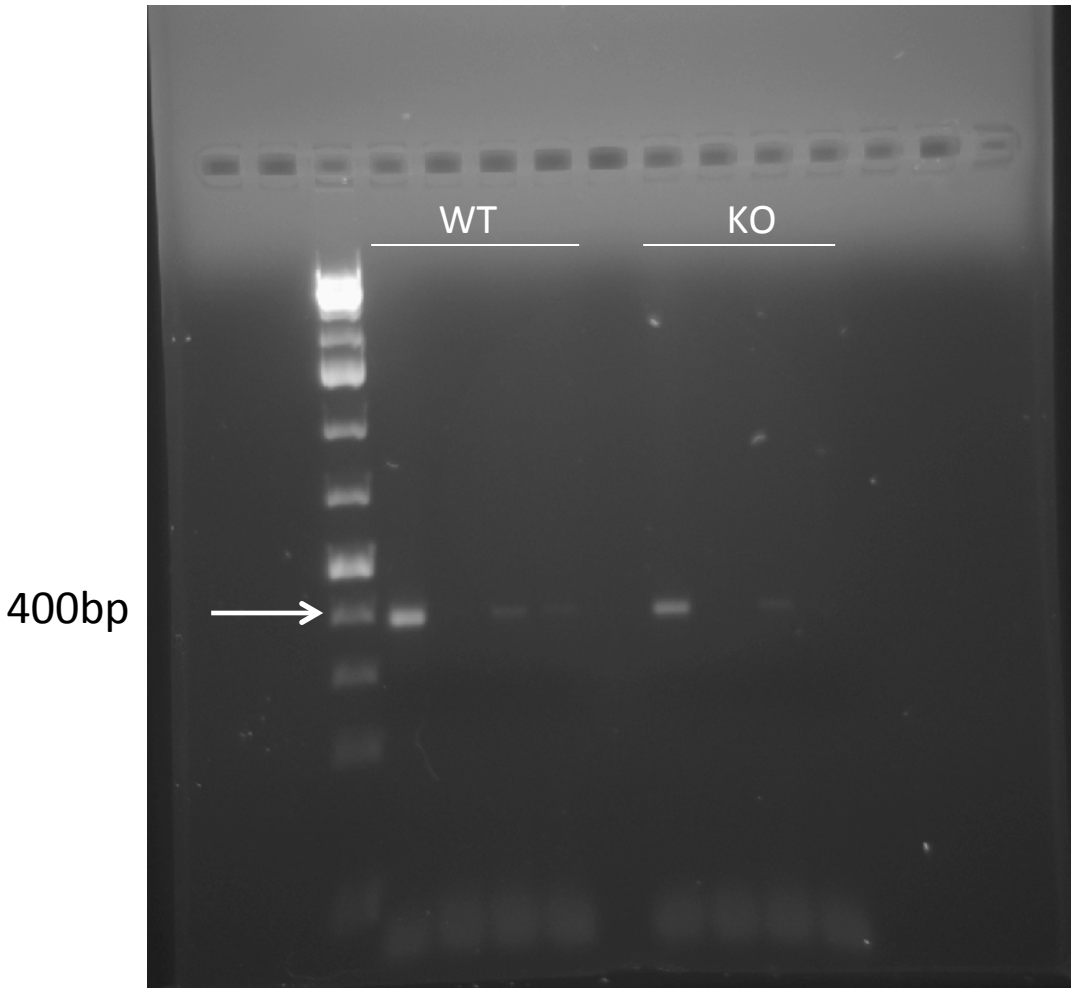

Figure 5D uncut gel

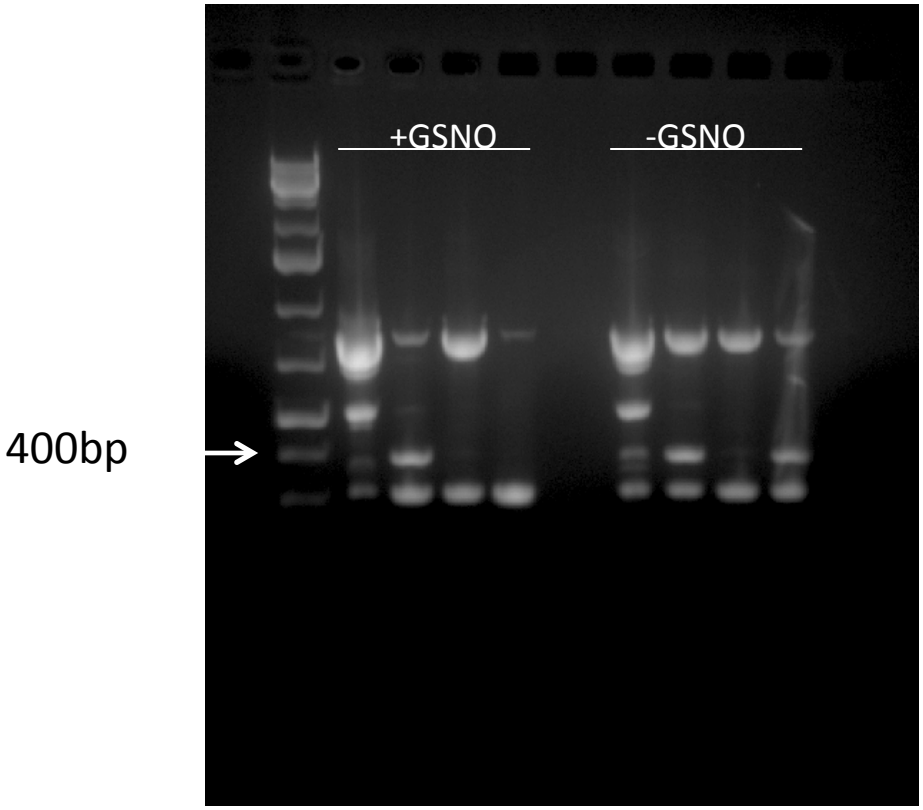

Figure 6D input uncut gel

Figure 6D pulldown uncut gel

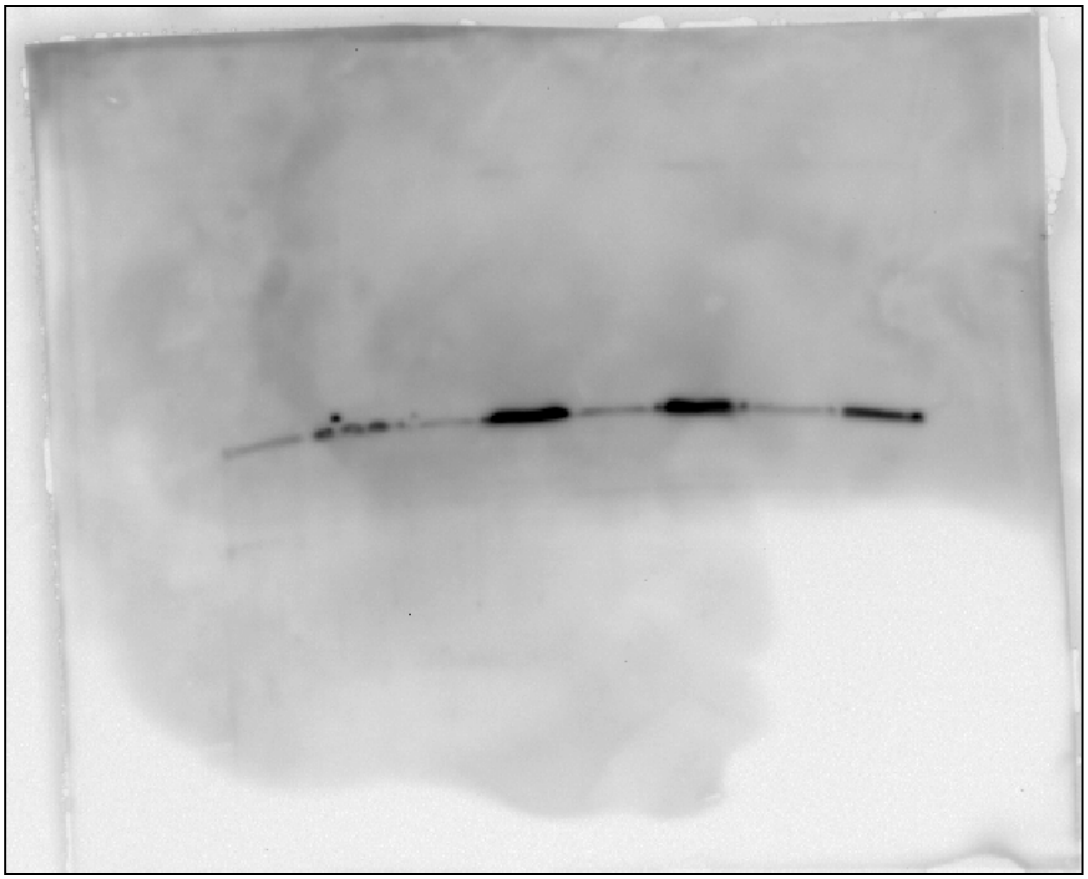

Figure S6A uncut gel

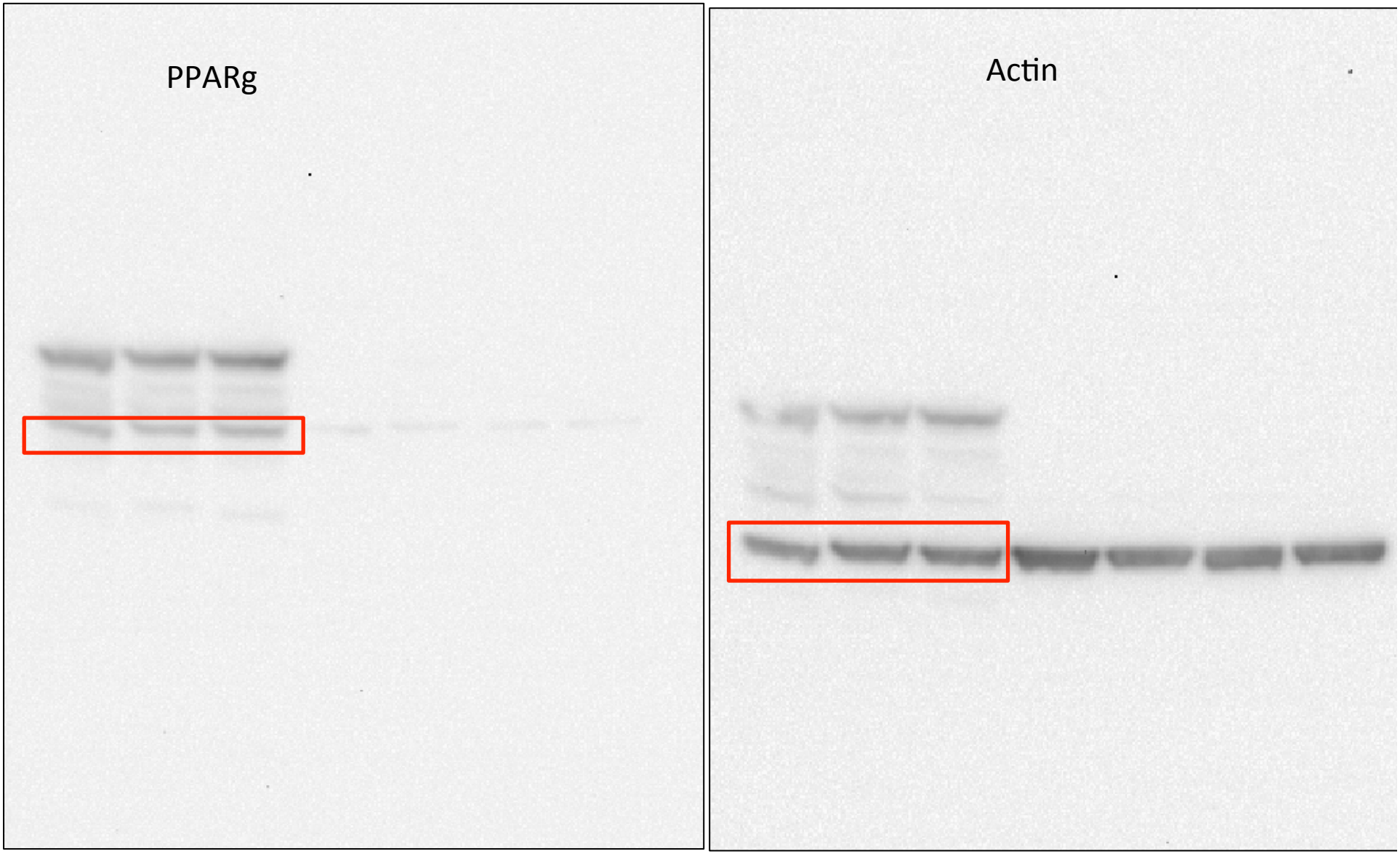

Figure S6B uncut gel

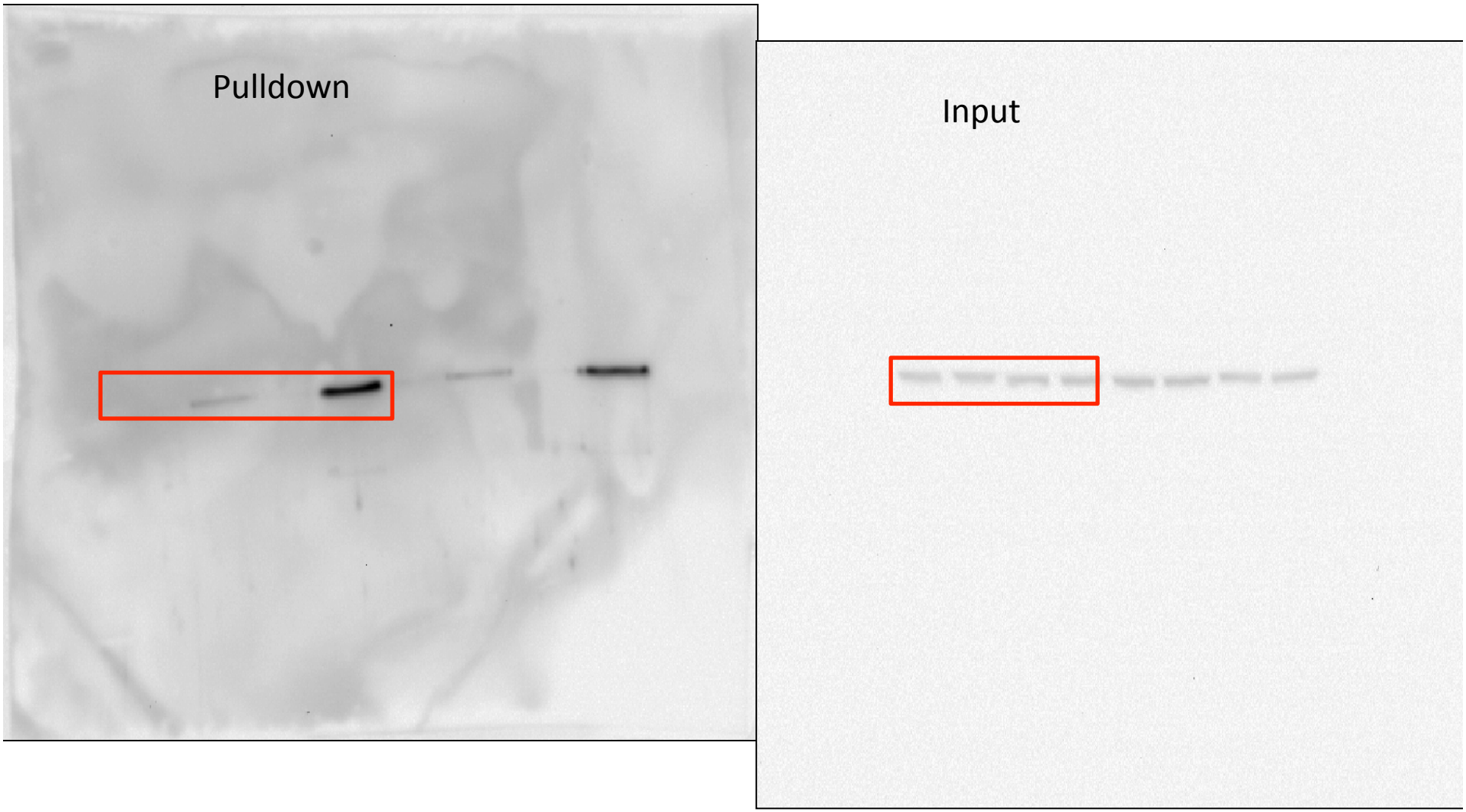

Figure S7A

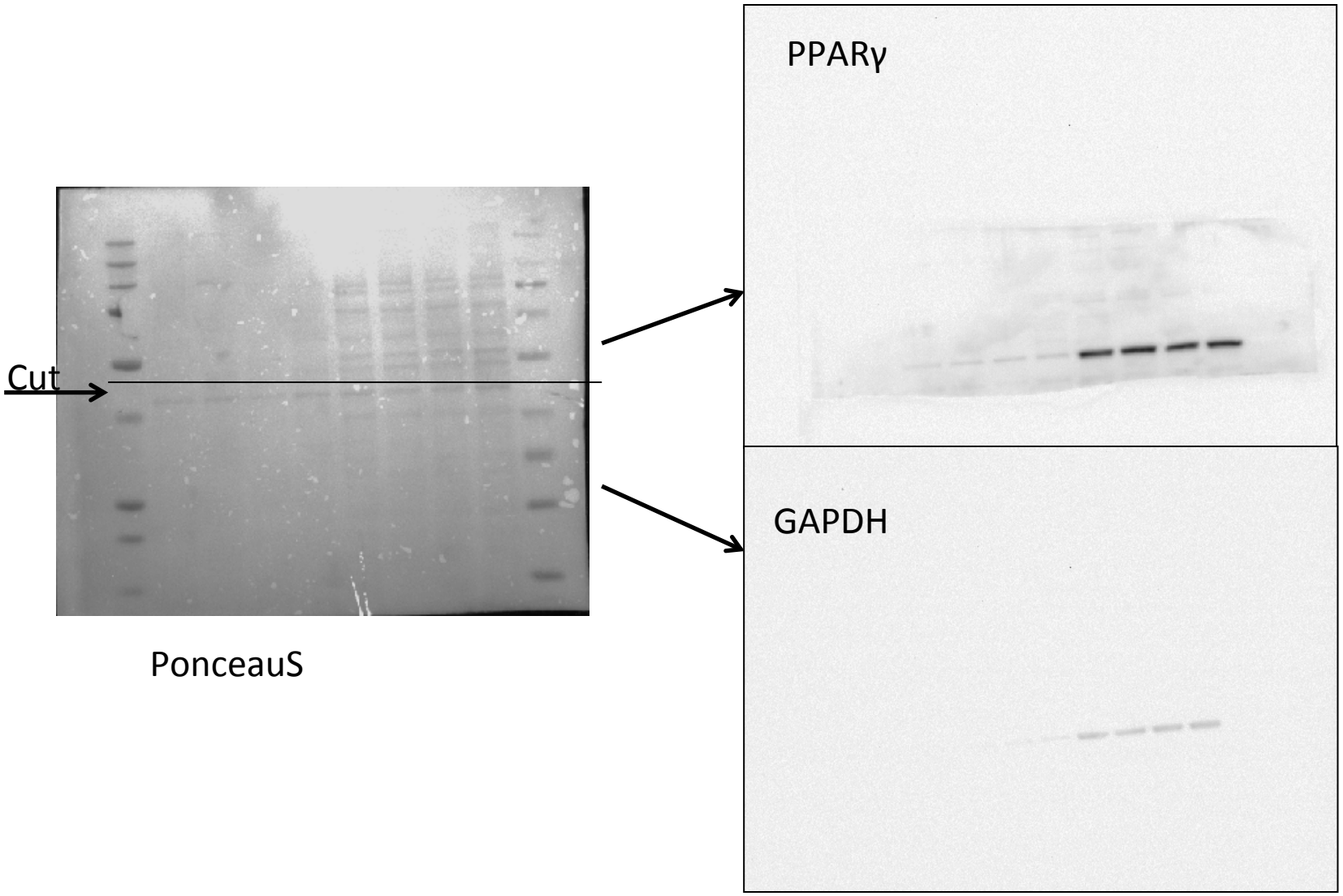

Figure S8A uncut gel

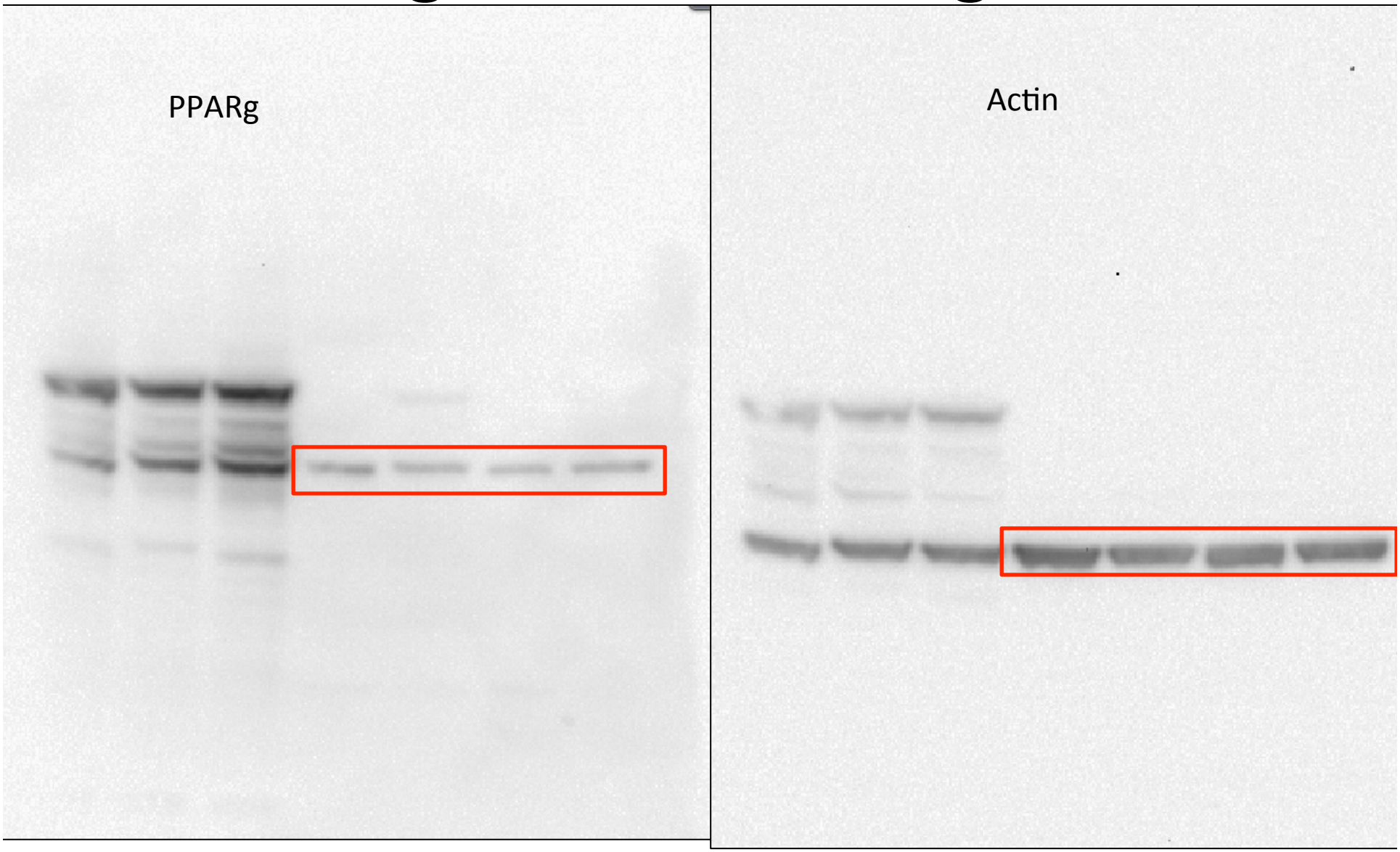

Figure S8B uncut gel

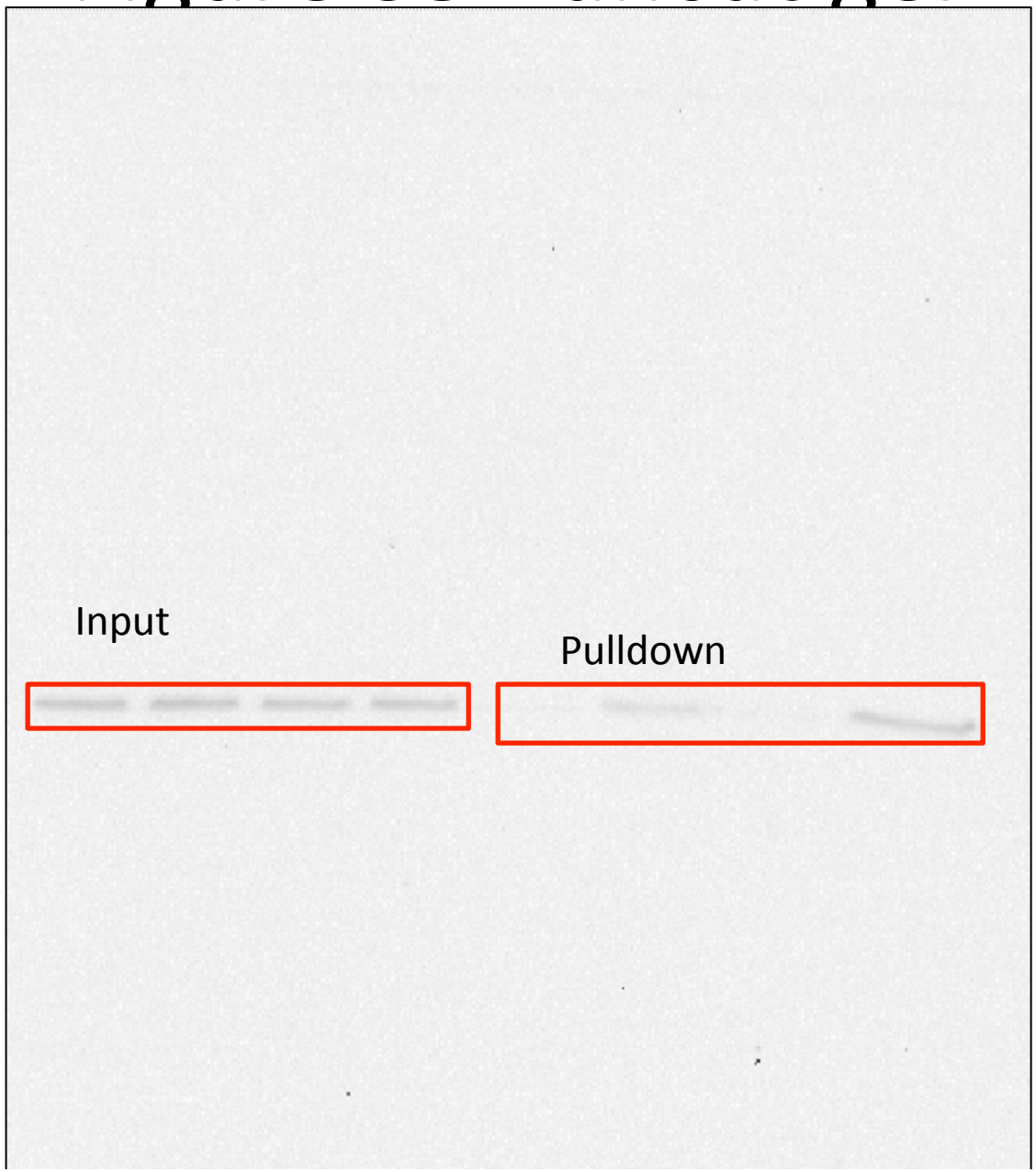

Figure S11 uncut gel pulldown

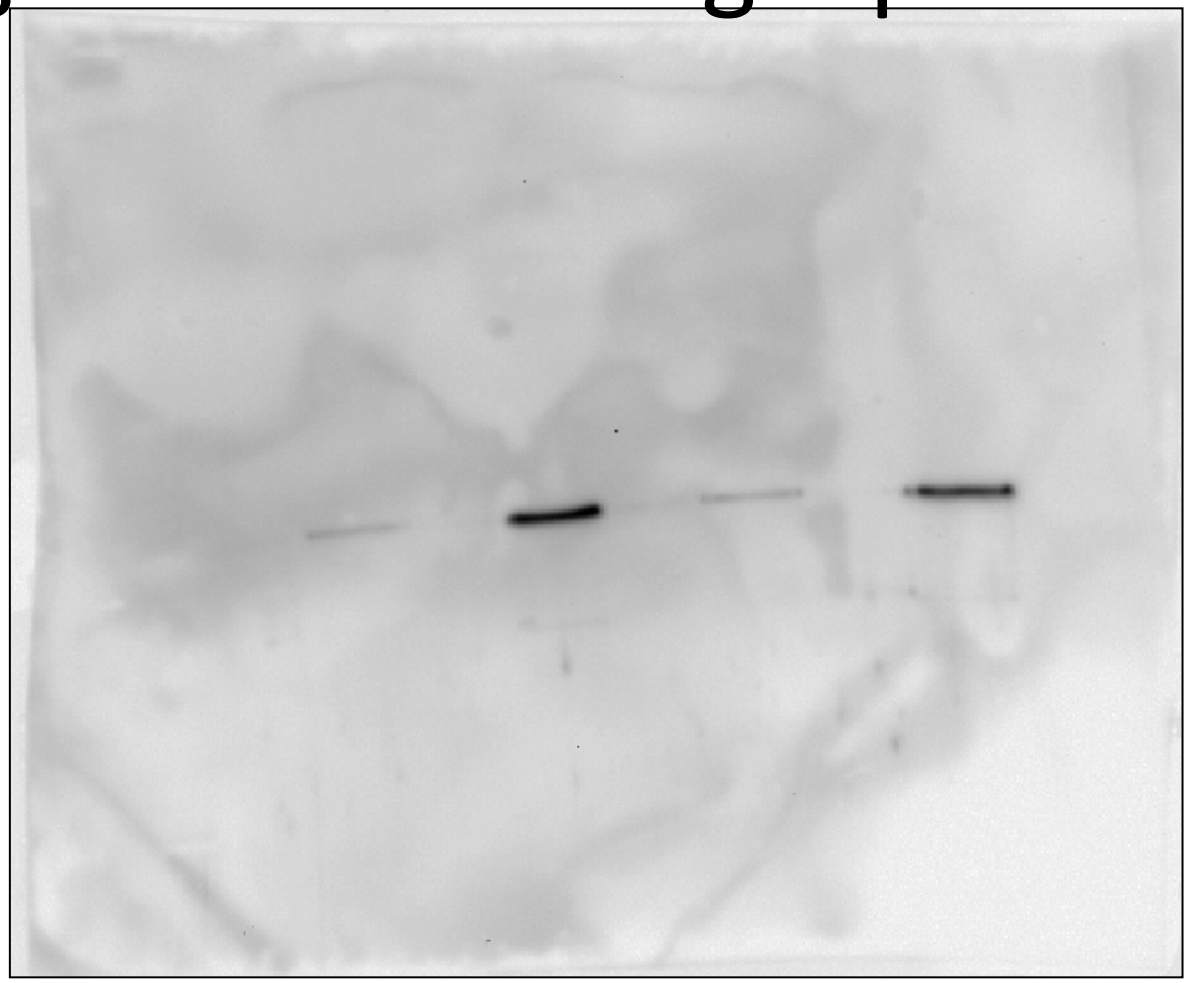

Figure S11 uncut gel Input